BNL-66703

MEASUREMENT AND MODELING OF SHORTWAVE IRRADIANCE COMPONENTS IN CLOUD-FREE ATMOSPHERES

R. N. Halthore
Environmental Chemistry Division
Department of Applied Science
Brookhaven National Laboratory
Upton, NY 11973-5000

July 1999

For publication in
Recent Research Developments in Geophysical Research,
S. G. Pandalai, Editor,
Research Signpost, Trivandrum, India, 1999.

Research by BNL investigators was performed under the auspices of the U.S. Department of Energy under Contract No. DE-AC02-98CH10886.

Measurement and Modeling of Shortwave Irradiance Components in Cloud-Free Atmospheres

Rangasayi Narayan Halthore

Brookhaven National Laboratory

ABSTRACT

Atmosphere scatters and absorbs incident solar radiation modifying its spectral content and decreasing its intensity at the surface. It is very useful to classify the earth-atmospheric solar radiation into several components - direct solar surface irradiance (E_{direct}), diffuse-sky downward surface irradiance ($E_{diffuse}$), total surface irradiance, and upwelling flux at the surface and at the top-of-the atmosphere. E_{direct} depends only on the extinction properties of the atmosphere without regard to details of extinction, namely scattering or absorption; furthermore it can be accurately measured to high accuracy (0.3%) with the aid of an active cavity radiometer (ACR). $E_{diffuse}$ has relatively larger uncertainties both in its measurement using shaded pyranometers and in model estimates, owing to the difficulty in accurately characterizing pyranometers and in measuring model inputs such as surface reflectance, aerosol single scattering albedo, and phase function. Radiative transfer model simulations of the above surface radiation components in cloud-free skies using measured atmospheric properties show that while E_{direct} estimates are closer to measurements, $E_{diffuse}$ is overestimated by an amount larger than the combined uncertainties in model inputs and measurements, illustrating a fundamental gap in our understanding of the magnitude of atmospheric absorption in cloud-free skies. The excess continuum type absorption required to reduce the $E_{diffuse}$ model overestimate (~3-8% absorptance) would significantly impact climate prediction and remote sensing. It is not clear at present what the source for this continuum absorption is. Here issues related to measurements and modeling of the surface irradiance components are discussed.

INTRODUCTION

Accurate measurement and estimation of shortwave irradiance components is a requirement to fully understand radiative transfer in the Earth-atmospheric system. The term 'shortwave' includes wavelengths in the solar spectrum between about 0.3 to 5 μm. Accurate measurement and calculation of the shortwave irradiance components along with those in the longwave (thermal infrared, >5 μm) are a priority activity for focussed field experiments and for meteorological monitoring around the world. Baseline Surface Radiation Network is an example of the latter wherein accurate measurements under a common protocol are continuously made at select stations around the world(1). Knowledge of the shortwave irradiance components under varying atmospheric and surface conditions is an integral part of studies of global energy budget and is required to be fully understood for application in such diverse fields as global climate prediction and remote sensing. Based on the estimates of the shortwave irradiance components, a number of recent studies have shown a significant discrepancy between calculated and measured atmospheric absorption in clear and cloudy atmospheres(2). The paper will address the comparisons between

measurements and model estimates of some of the shortwave irradiance components in cloud-free atmospheres using data from an ongoing field experiment in mid-continental North America.

The components of shortwave irradiance are, with increasing level of complexity, direct-normal solar irradiance at the surface (E_{direct}), diffuse downward surface irradiance ($E_{diffuse}$), global or total surface irradiance (E_{total}), upwelling flux at the surface ($E^{\uparrow}_{surface}$) and upwelling flux at the top-of-the atmosphere ($E^{\uparrow}_{TOA}$). Among these, E_{direct} is the simplest component as it depends only on the solar irradiance at the top of the atmosphere and the atmospheric attenuation (transmittance) along the path from the Sun; it does not depend on the proportion of scattering and absorption in total attenuation. To first order, $E_{diffuse}$ depends on the atmospheric scattering by molecules and aerosols. To a lesser extent, it depends on the surface reflectance and, if the atmospheric aerosol content is high, on the surface – atmospheric coupling of radiation. E_{total}, like $E_{diffuse}$, depends to second order on surface reflectance. A closure experiment (comparison between modeled and measured values) in E_{total} is more difficult than in $E_{diffuse}$ because E_{total} measurement is subject to larger uncertainties. For both $E_{diffuse}$ and E_{total} it is normally sufficient to assume that reflectance is both isotropic (Lambertian) and uniform. For $E^{\uparrow}_{surface}$ a more realistic description of surface reflectance may be necessary. This leads to complications because it is not easy to measure bi-directional reflectance distribution function (BRDF) for every case in a field experiment. Assumptions simplifying characterization of surface reflectance lead to potentially large errors in estimates of $E^{\uparrow}_{surface}$. Of all the irradiance components, $E^{\uparrow}_{TOA}$ is the most complicated as its measurement is most difficult and its model calculation, most uncertain. Atmospheric absorptance, a key parameter, requires an estimate of $E^{\uparrow}_{TOA}$ and other components and therefore is subject all the uncertainties in the estimates of these components. Below relevant quantities are first defined.

Definitions

Direct-normal solar irradiance, E_{direct} (W m^{-2}), is defined as the solar energy incident per unit time on a unit area normal to the Sun's direction at the surface. E_{direct} depends on the extra-terrestrial solar energy and the atmospheric transmittance. It is expressed in terms of spectral solar extra-terrestrial irradiance, E_o^{λ} in W m^{-2} μm^{-1} at 1 Astronomical Unit (A.U.), and spectral transmittance, T^{λ}, as,

$$E_{direct} = \left(\frac{1}{R^2}\right)\int E_0{}^{\lambda} T^{\lambda} d\lambda, \qquad [1]$$

where R is the Sun- Earth distance in A.U. The integration is performed over the entire solar spectrum between about 0.3–5 μm. In a cloud-free atmosphere molecular scattering (Rayleigh scattering), gaseous band and continuum absorption, and aerosol scattering and absorption, cause extinction along the direct path from the Sun. Spectral transmittance T^{λ} can be written as a product of contributions from molecular scattering ($T^{\lambda}_{Rayleigh}$), molecular or gaseous absorption (T^{λ}_{gas}) and aerosol scattering and absorption ($T^{\lambda}_{aerosol}$) as,

$$T^{\lambda} = T^{\lambda}_{Rayleigh}.T^{\lambda}_{gas}.T^{\lambda}_{aerosol}. \qquad [2]$$

Accurate estimates of solar spectral irradiance and measurements of atmospheric transmittance are required for an accurate calculation of E_{direct} using equation 1. E_{direct} is insensitive to surface reflectance. A comparison of measured and modeled E_{direct} leads to a simple and robust closure experiment, one that evaluates the solar spectrum and the transmittance incorporated into the models. It is simple because distinction between scattering and absorption in total attenuation need

not be made in model estimates (nor can it be made in measurements); it is robust because E_{direct} can be accurately measured.

Diffuse Downward Irradiance, $E_{diffuse}$ (W m^{-2}), is the surface irradiance from the hemispherical sky arising due to the solar energy scattered by atmospheric molecules (Rayleigh scattering) and aerosols. It does not include the vertical component of E_{direct}. Although exact analytical expressions for radiance L (W m^{-2} Sr^{-1} μm^{-1}) as a function of view zenith angle, θ_v, and the view azimuth angle, ϕ_v, can be obtained under single scattering approximation, for realistic computation of sky radiance multiple scattering must be included. This is clearly apparent in Figure 1 where the results of model computations for assumed atmospheric conditions and overhead Sun are shown for three cases – single scattering, 2-stream and 8-stream multiple scattering. In this figure, atmospheric radiance at 550 nm in W m^{-2} Sr^{-1} μm^{-1} is plotted as a function of view zenith angle. The difference between single scattering and multiple scattering computations are greater for zenith angles higher than 40˚. Therefore, for a more realistic description of the radiation field, 2-stream or better yet, 8-stream multiple scattering computations should be performed, especially for atmospheres with large aerosol extinction. All curves in Figure 1 show a minimum at 50 degrees and increase toward larger zenith angles due to longer path lengths and, to a smaller extent, the surface – atmospheric coupling. The latter refers to the phenomenon of multiple reflections between the atmosphere and the surface, important for high surface reflectance and high aerosol content in the atmosphere.

Radiance L computed by a model and shown in Figure 1 is integrated to obtain spectral surface irradiance, $E_{diffuse}(\lambda)$ thus,

$$E_{diffuse}(\lambda) = \iint_{\theta_v,\phi_v} L(\theta_v,\phi_v,\lambda)\sin\theta_v\cos\theta_v d\theta_v d\phi_v, \quad \theta_v,\phi_v \neq \theta_0,\phi_0. \quad [3]$$

$E_{diffuse}$ is obtained by integrating $E_{diffuse}(\lambda)$ over the solar spectrum. View angles corresponding to solar zenith angle θ_0, solar azimuth angle, ϕ_0, represent direct irradiance. Although radiance as seen in Figure 1 increases for large zenith angles, the contribution to flux from those angles is small. This can be seen in a computation of fractional flux or irradiance defined here as the flux or irradiance due to the radiance within each ten degrees of zenith distance from 0 to 90˚ computed according to equation (3). Result shows (Figure 2) that the fractional flux contribution from zenith angles between 80 and 90˚ is a mere 6% of the total $E_{diffuse}$ at 550 nm.

Parameters that affect the magnitude of scattered light include the vertical optical thickness, τ_0, a measure of total extinction (note: $T = e^{-\tau_0/\mu}$, where T is the transmittance and μ is the cosine of zenith angle), single scattering albedo, ω_0, defined as the ratio of scattering to total extinction and phase function, p, defined as the fraction of scattered light into a unit solid angle in a given direction. It is often convenient to specify the asymmetry parameter, g, defined in terms of phase function p as(3),

$$g = \left(\frac{1}{2}\right)\int_{\mu=-1}^{1} p(\Theta)\mu d\mu \quad [4]$$

where μ is cos(Θ). Phase function for Rayleigh scattering is symmetric with g=0. For aerosols that are much larger than molecules and comparable in size to the wavelength of light, forward scattering is predominant (g ~0.6).

Global or Total surface irradiance, E_{totab} (W m^{-2}) is the sum of $E_{diffuse}$ and the vertical component of E_{direct}. If θ_0 is the solar zenith angle,

$$E_{total} = E_{direct}.\cos(\theta_0) + E_{diffuse}. \quad [5]$$

Under cloud-free conditions the direct component dominates.

Upwelling flux at the surface, $E^{\uparrow}_{surface}$, and at the top-of-atmosphere, $E^{\uparrow}_{TOA}$ (W m^{-2}) are most sensitive to surface reflectance. For a surface with a reflectance $\rho(\lambda)$ that is Lambertian (isotropic) and uniform, $E^{\uparrow}_{surface}$ is given by,

$$E^{\uparrow}_{surface}(\lambda) = \rho(\lambda) E_{total}(\lambda). \quad [6]$$

At the TOA, if L_{TOA} is the radiance at an angle (θ_v, ϕ_v) for solar illumination at (θ_0, ϕ_0), then (4)

$$L_{TOA} = L_0 + \left(\frac{E_d}{\pi}\right)\left(\frac{\rho}{1 - s\rho}\right)T, \quad [7]$$

where for all quantities dependence on λ is omitted for convenience. L_0 is the atmospheric path radiance arising from photons that are scattered directly from the atmosphere without interacting with the surface, E_d is the surface irradiance for zero surface reflectance, T is the transmittance, s is the atmospheric reflectance and the term containing s and ρ in the denominator is the correction to account for the surface – atmospheric coupling. $E^{\uparrow}_{TOA}$, is obtained by integrating L_{TOA} over all viewing directions (analogous to equation 3) and over all wavelengths. Real surfaces are neither uniform nor Lambertian; their reflectance is best characterized by the BRDF(5). $E^{\uparrow}_{TOA}$ constitutes the most complex of the radiation components considered here as it depends on surface reflectance and atmospheric scattering including back scattering.

For the various shortwave radiation components, the equations above are written to illustrate the definition of the above quantities; models do not necessarily compute these quantities according to these equations.

Atmospheric absorption in terms of the measurements or model estimates of the components of shortwave irradiance is given by,

$$Absorptance = \frac{(E_{total,TOA} - E^{\uparrow}_{TOA}) - (E_{total} - E^{\uparrow}_{surface})}{E_{total,TOA}}. \quad [8]$$

Here absorptance is expressed as a fraction of the incoming shortwave irradiance at the top of the atmosphere, $E_{total,TOA}$. Atmosphere absorbs solar energy only in its sunlit hemisphere at an average solar zenith angle of 60˚. Measuring or computing the irradiance components at a solar zenith angle of 60˚ will then permit estimate (using equation 8) of absorptance of sunlit hemisphere. Global average absorbed power (W m^{-2}) is obtained by multiplying absorptance by the global average solar irradiance (342 W m^{-2}, see below). The above procedure for determining atmospheric absorption is typically applied to either cloud-free or cloudy skies.

Measurement of irradiance components

Direct normal solar irradiance, E_{direct}

E_{direct} is measured using pyrheliometer and active cavity radiometer (ACR). Both these instruments use thermopile detectors but the method of operation is substantially different. In the ACR, electrical power is supplied to heat a reference cavity to compensate for or "balance" heating of active cavity by radiant energy. The amount of electrical energy supplied is proportional to the amount of radiant energy falling on the ACR thus providing an absolute irradiance calibration. Radiometers of this type are also called "electrical substitution radiometers" and can be calibrated to high accuracy, ~0.3% (at the 3-sigma level(6)). A group of seven such radiometers, called the World Standard Group, with well characterized long term response, form a core group of instruments maintaining absolute irradiance standard called the World Radiation Reference (WRR) standard at the World Radiation Center at Davos, Switzerland. In the pyrheliometer, the radiant energy input produces a proportional output voltage, which is calibrated against ACR(s). Due to drift in the thermopile detector response,

accuracy is ~2% which can be reduced considerably by calibrating pyrheliometers frequently throughout the duration of a field experiment.

Sun is observed with a narrow field-of-view collimator (~5˚) large enough to completely include Sun's disc in the field-of-view, but small enough to exclude much of the scattered radiance from the Earth's atmosphere. The field-of-view is larger than the solar disc (Sun subtends approximately 0.5˚) to accommodate small errors in scanning throughout the day and therefore includes some sky brightness in addition to direct irradiance. The intensity of light in the solar aureole (in the region very near the Sun) is a function of the amount and size distribution of aerosols; larger the aerosols, brighter the aureole because of increased forward scattering. A correction for the aureole brightness is calculated to be approximately 0.1% of solar irradiance(7). An example of E_{direct} measured using a pyrheliometer on a cloud-free day is shown in Figure 3. The variability seen here is due to fluctuations in transmittance – most likely aerosol optical thickness, $\tau_{aerosol}$. In fact, it is observed that measured E_{direct} is anti-correlated with fluctuations in $\tau_{aerosol}$.

Downward irradiance at the surface

Downward irradiance from the hemispheric sky is measured by a pyranometer consisting of flat, blackened, thermopile detector. The detector is mounted on a base and covered by hemispherical glass dome(s). A perfect detector will have an ideal cosine response to light striking the horizontal surface at various angles but this is never achieved in practice. If energy from a source that subtends a narrow angle at the detector contributes a constant direct-normal irradiance E then the detector with an ideal cosine response will have an output that is proportional to $\cos(\theta)$ where θ is the angle between the normal to the detector and the source (zenith angle). In cloud-free conditions, bulk of the energy in the total hemispherical sky irradiance is in the direct beam. Thus, small deviations from the ideal cosine response will have relatively large effects on the measured total irradiance.

Diffuse irradiance is measured by a shaded pyranometer when the Sun is blocked either with a shadowband (a metal band along apparent daily Sun's path and wide enough to obscure the Sun) or with an occulting disc (circular in shape) that is Sun-synchronous. Shadowband obscures the Sun throughout the day but it also obscures large portions of the sky amounting to a correction of 4% of diffuse irradiance. A shadow disc blocks the Sun and the aureole but not much else; a correction in this case is about 2%. Because the diffuse sky brightness is relatively uniformly distributed in a cloudless sky compared to the non-uniform distribution of brightness in total irradiance, errors due to the non-ideal cosine response are minimized. It is for this reason that the generally accepted procedure for obtaining total surface irradiance is to add the vertical component of direct normal solar irradiance E_{direct} measured by an ACR or a pyrheliometer to the diffuse irradiance $E_{diffuse}$ measured by shaded pyranometer(1,8). In Figure 3 total and diffuse surface irradiance measured by an unshaded and shaded pyranometer are shown for the same cloud-free day as for the direct irradiance measurement. The measured diffuse irradiance never exceeds 50 W m^{-2} indicating that the aerosol content in the atmosphere is low for this day and that there are no clouds in the sky. The diffuse irradiance is highly sensitive to the presence of clouds.

Calibration of pyranometers is more complicated than that of pyrheliometers owing to the difficulty in determining the amount of energy falling on the detector during calibration. To circumvent this, pyranometers are calibrated by the so-called shade/unshade technique wherein the response of pyranometers to direct normal solar irradiance is compared with ACR measured values. In this shade/unshade technique, also known as the sun-

disk technique(9), the pyranometer is alternatively shaded and unshaded to obtain by difference of total and diffuse irradiance, the vertical component of direct-normal irradiance, which is then compared to the vertical component of E_{direct} measured by an ACR. Alternatively, for cases when an ACR is not available(9,10), a reference pyranometer itself calibrated by the sun-disk technique against ACRs of the WRR could be used as the basis of calibration of field pyranometers.

Use of shade/unshade technique involves taking difference of instrument responses for two irradiance levels. Bias information is therefore lost(11). Because of this, pyranometers are seen to depict (Figure 4) negative values at night when the shortwave irradiance is zero. Furthermore, at the time of sunrise and sunset indicated (Figure 4) by a rapid rise in the E_{direct} as measured by the pyrheliometer, the diffuse light level is found to be negative when it ought to be positive; it is a common observation that the daylight persists about 15 minutes beyond sunrise or sunset into the night. This nighttime offset is thought to arise from instrument cooling to the atmosphere. In Figure 5 are plotted two data points, one in the morning and one in the evening for a purely Rayleigh atmosphere. The uncorrected diffuse irradiance curve (same as in Figure 4) is below these two points which is impossible since diffuse irradiance due to Rayleigh scattering represents a minimum(12). Clearly diffuse irradiance must be corrected for negative offsets.

Negative nighttime values and by implication daytime offsets, can be substantial fraction of measured daytime diffuse irradiance (Figure 5). Accurate determination of diffuse irradiance being a priority activity, much effort is focussed on methods to ascertain the magnitude of the daytime offsets. At a minimum a simple or interpolated subtraction of the observed nighttime offsets from the daytime values appears to be necessary(13). The result of a such a correction is shown in Figure 5, where now the corrected diffuse irradiance can be seen to be above the Rayleigh limit. Use of surrogates for instrumental cooling such as the net longwave downward irradiance as measured by an up-looking pyrgeometer (a device much like the pyranometer but one that measures longwave or thermal radiation) has long been recommended (private communication, Dr. Ellsworth G. Dutton, U.S. National Oceanic and Atmospheric Administration, Boulder, Colorado). This is accomplished first by obtaining a correlation between observed nighttime net-longwave downward irradiance and nighttime offsets, and second, by applying the same correlation for daytime longwave irradiance measurements to calculate daytime offsets(11). Other methods that are based on measured base and dome temperatures in pyranometers or pyrgeometers have been proposed and are being investigated (B. Forgan, private communication and reference(14)).

Experience with a large number of pyranometers shows that the uncertainty in measurement of diffuse irradiance is ±5 W m^{-2} at the 75% confidence limit and ±8 W m^{-2} at the 95% confidence limit. This is clearly much larger than measurements using ACRs which differ from each other typically by about 1 W m^{-2} in a measurement of 1000 W m^{-2}.

Upward Irradiance at the surface and at the TOA

Measurement of upward flux at the surface and at the TOA involves reorientation of the unshaded pyranometer to a downward looking configuration. All instrumental and calibration issues remain the same as for the shaded pyranometer case since only the diffuse light is measured. An additional complication for measurement at altitude is the alignment on unstable or moving platforms such as aircraft.

Satellite measured radiance is frequently used to estimate $E^{\uparrow}_{TOA}$(15). The procedure involves estimating broadband flux from narrow-band

fluxes since satellites typically measure radiance in narrow channels. An issue also is the conversion of satellite measured radiance to flux; most satellites sample the radiance field with one set of viewing angles. Presence of non-Lambertian, non-uniform reflectance fields in the scene due to clouds for example, complicates such a determination of TOA flux. Also when used in conjunction with in situ measurements at the surface, accuracy in pixel co-location is a factor; some averaging may be necessary.

Models, model inputs and measurement of model inputs

MODTRAN is a widely used medium resolution (2 cm^{-1}) radiative transfer model developed by United States Air Force Geophysical Laboratory at Hanscom Air Force Base(16,17,18). It uses parameterizations for gaseous absorption that are common to many other codes used either independently or embedded in other models such as General Circulation Models. MODTRAN employs three algorithms for solving the transfer equation that allow computation of radiance and flux – a single scattering model, a two stream approximation and a multi-stream model based on a discrete ordinate method. A sample of the results of the three algorithms is shown (Figure 1) and already discussed above. Although the difference in calculated radiance among the models for the same inputs is large in Figure 1, difference in flux calculations is smaller. This is due to the conservative nature of scattering applicable for cases when the atmospheric absorption is low; the missing photons from a particular region of the sky manifest in some other region.

Solar Spectrum

A high-resolution solar spectrum(19) consistent with the data of Neckel and Labs(20) is available in MODTRAN. The integrated value (solar constant) of this adopted solar spectrum is 1373.2 W m^{-2} at 1 astronomical unit, slightly higher than 1366 ± 3 W m^{-2}, average of satellite observations in the last 15 years(21).

Atmospheric transmittance

Transmittance due to Rayleigh scattering is well known and is expressed as a function of surface pressure and wavelength. Surface pressure is either directly measured or is estimated by assuming an atmosphere under hydrostatic equilibrium to good accuracy ($\Delta\tau < 0.005$ where $\Delta\tau$ is the uncertainty in vertical optical thickness(22)). Molecular absorption by well-mixed gases (such as carbon dioxide) is proportional to the absorption coefficient determined at the wavelength resolution of the model and the climatological abundance. For MODTRAN, molecular band parameters are computed from the AFGL HITRAN database, a comprehensive molecular database compiled from models and observations(23). For variable gases and vapors (example, ozone and water vapor), abundance is determined either from observations (radiosonde in case of water vapor and satellite measurements in case of ozone) or from climatology (ozone).

In addition to the band absorption by gases, which are relatively well known, models also need to include continuum and other wavelength structured absorption. Presence of water vapor continuum in the thermal infrared(24) is well known and many models (including MODTRAN) include it. Quasi-continuum absorption by NO_2 in the visible is also relatively well known (25,26). Structured absorption in the shortwave by collision pairs involving O_4, O_2-N_2, and other trace gases (including water dimer) contribute a small but significant amount to the overall shortwave absorption by gases(27,28). Continuum absorption in the shortwave could arise from obvious sources - overlapping of far wing absorption, dimer and trimer transitions, transitions in a compound molecule such as H_2O-N_2, H_2O-O_2 and other combinations with trace gases. Another source of continuum absorption is

the absorbing aerosol, which is obviously variable. Continuum absorption in the shortwave is a topic of current interest, one that has implications for closure in shortwave irradiance components.

Sunphotometry and the measurement of total optical thickness

Aerosol extinction and water vapor absorption constitute the most variable components of atmospheric extinction or optical thickness. Aerosol extinction is a major source of uncertainty in computations of the components of shortwave radiation(22). Using a technique that can be traced to Bouguer(29), sunphotometers directly measure optical thickness without the need to calibrate them for absolute irradiance. The technique, commonly termed as the Langley plot method or the Long Bouguer method, can be best illustrated with the aid of Bouguer's law (or as is commonly known, Beer-Lambert-Bouguer law). E_{direct} can be expressed as,

$$E_{direct} = \left(\frac{E_0}{R^2}\right)T = \left(\frac{E_0}{R^2}\right)e^{-(m\tau)_{total}}$$

where m is the airmass ($\cong \sec\theta$, $\theta$is the zenith angle), E_0 is the extra-terrestrial direct normal solar irradiance referred to 1 A.U., T, the total transmittance is expressed in terms of the total vertical optical thickness, τ_{total}, comprising of Rayleigh scattering, gaseous absorption and aerosol scattering and absorption. If the instantaneous instrument response to E_{direct} is voltage V,

$$V = \left(\frac{V_0}{R^2}\right)\exp\left[-(m\tau)_{Rayleigh} - (m\tau)_{ozone} - (m\tau)_{aerosols}\right] \quad [9]$$

where V_0 is the response to E_0. It is assumed that each component of extinction can be explicitly identified. The above equation is the basis of optical thickness (and hence transmittance) measurement provided the calibration coefficient V_0 is known. A plot of $\left[\ln(V) + (m\tau)_{Rayleigh} + (m\tau)_{ozone}\right]$ versus airmass m, termed Langley plot, obtained under clear and stable conditions, during periods of maximum airmass change such as those during mornings or evenings, yields a straight line provided the apparent aerosol optical thickness ($\tau_{aerosol}$) is constant. The y-intercept of this Langley plot, is $\left[\ln\left(V_0 / R^2\right)\right]$ from which the required calibration coefficient V_0 is determined; the slope is $\tau_{aerosol}$. The calibration coefficient V_0 determined this way is used in equation [9] to obtain an instantaneous measurement of $\tau_{aerosol}$ using equation [9]. If gaseous absorption is not completely known in a given sunphotometer channel, the ordinate of the Langley plot may just include *ln V*. The slope of the Langley plot would then be the total optical thickness.

Sunphotometers are narrow field-of-view (FOV) devices that sample the direct normal solar irradiance with the aid of a silicon detector in narrow channels throughout the visible and near-IR regions of the solar spectrum. The FOV is typically ~1˚ reflecting the fact that they position or capture the Sun's image more accurately than the pyrheliometer within the FOV. For automatic devices, accurate positioning is possible because of the use of quadrant detectors in a feedback control loop. For manual (handheld) devices, accurate capturing of the image is possible by the use of "peak hold" feature that enables electronically registering maximum voltage. The excellent repeatability and linearity of silicon detectors allows calibration to very high accuracy. Filter degradation due to humidity and high intensity is the main cause of deterioration of instrument performance but recent developments in filter manufacturing technologies have improved the stability in instrument response considerably. Thus, the Langley plot method of calibration under excellent atmospheric conditions such as those found on top of Mauna Loa, Hawaii, in conjunction with superior instrument construction can yield calibration coefficients to an accuracy better than 0.01 in optical

thickness(30). Measurements of optical thickness with well-calibrated sunphotometers usually agree to within 0.01 of each other(31).

For an estimate of E_{direct}, partitioning of extinction into its components - scattering and absorption - is not required. In addition, models used to estimate extinction in sunphotometry and in the computation of E_{direct} are essentially same. For model computation of E_{direct} sunphotometer measured transmittance in narrow wavelength bands throughout the visible and near-IR is required as input; the model then has to compute transmittance in between and beyond sunphotometer channels. The integrated value of the transmittance is therefore model dependent.

Aerosol scattering properties

At wavelengths in the shortwave, aerosol single scattering albedo and phase function (alternatively, asymmetry parameter) are required for the computation of all shortwave radiation components except E_{direct}. Two approaches are taken – one that characterizes the microphysical and chemical properties of the aerosols such as size distribution, shape and composition of the aerosols and the other that directly measures the required optical properties. In the latter, more practical approach, one that is followed in most field experiments, nephelometers measure the scattering and hemispheric backscattering coefficients(32,33) from which g is calculated(34). Measurement of absorption coefficient is accomplished using an integrating plate method(35) or variations thereof(36); ω_0 can then be estimated. Because air streams are dried in nephelometers to about 30% relative humidity (RH) or lower, the measured ω_0 is the lower limit. Uncertainty is generally assumed to be ~10%.

Surface reflectance

Surface reflectance measurements have long been performed in support of satellite data validation and calibration. For shortwave energy budget studies, full and accurate characterization of surface reflectance (BRDF) is required but rarely carried out in practice. This is because the procedure involves measurement of radiance above the same surface at all possible angles, wavelengths, and solar zenith angles, in addition to simultaneously extending this set of measurements to adjacent sites - quite a tedious and impractical procedure. Instead, two practical approaches are employed based on whether it is better to assume isotropic but non-uniform surface reflectance or non-isotropic but uniform surface reflectance. In the former case, nadir measurement of radiance are rapidly made over large areas using an aircraft or helicopter based radiometer; even handheld, nadir pointing spectro-radiometers are used on smaller areas. In the latter case, instruments that rapidly acquire multi-angle, multi-wavelength radiance above a uniform surface are employed to characterize the reflectance(37).

RESULTS AND DISCUSSION

Models calculate E_{direct} to within uncertainties in measurement and model estimates

MODTRAN 3 calculates instantaneous E_{direct} to within 0.012 ± 0.45% of measured values (Figure 6; also reference (7)). This accuracy is achievable because of the accurate estimation of instantaneous $\tau_{aerosol}$ in discrete channels throughout the visible and near-IR using the sunphotometer, accurate measurement of atmospheric water vapor and temperature with height using the radiosonde at the time of the irradiance measurement, accurate estimate of ozone column abundance from climatology (and checked with satellite data) and accurate measurement of E_{direct} using ACRs and pyrheliometers calibrated with ACRs.

Results (7) from a mid-continental site in United States of America (Southern Great Plains (SGP) site in Oklahoma) were analyzed with over 30

individual cases of comparisons. Recently many more comparisons (Figure 6 and reference (13)) at SGP and at other sites including some high altitude sites have confirmed the above findings. In addition to SGP, these sites include low altitude sites in the boreal forest in mid-continental Canada (BOREAS in Saskatchewan and Manitoba), a high altitude site on Mauna Loa, Hawaii (MLO), and a high altitude site at the South Pole, Antarctica (SPO). Sensitivity analysis shows that an uncertainty in sunphotometer measured optical thickness of ±0.01 (the dominant term) translates to about 1.6% uncertainty in E_{direct}. A combination of ±0.01 uncertainty in optical thickness along with 10% in precipitable water, 0.1 in Angstrom exponent (b in $\tau_{aerosol} \sim a\lambda^{-b}$, where λ is the wavelength), 20% in ozone column abundance and 0.3% in E_{direct} measurement leads to an uncertainty of 1.8% in the difference between modeled and measured E_{direct}, provided the uncertainties in the above quantities are uncorrelated. The actual discrepancy between modeled and ACR measured E_{direct} of 0.012% ± 0.45% for 11 comparisons and pyrheliometer measured E_{direct} of –0.4% ± 0.82% for 49 comparisons (Figure 6) is much less than this combined uncertainty making this a successful closure experiment. Even better agreement between modeled and measured E_{direct} can be obtained if ozone column abundance is determined to better accuracy at the time of comparison.

It was concluded that since MODTRAN is capable of accurately estimating E_{direct} our knowledge of solar spectrum and atmospheric transmittance, at the resolution of the model (2 cm^{-1}), is complete. It was further concluded (erroneously it turns out, see below) that since all contributions to atmospheric extinction are well understood, the amount of atmospheric absorption is also well represented in the model. For a standard mid-latitude cloud-free atmosphere, MODTRAN calculates about 21% absorptance which is close to the generally accepted 'text book' value of ~20% absorptance(38). Efforts are underway at present to perform a model intercomparison to determine if many of the commonly used models do agree with one another and with measurements in computing E_{direct}, thereby validating their use of the solar spectrum and atmospheric transmittance in the shortwave.

Models overestimate $E_{diffuse}$

Closure in $E_{diffuse}$, in contrast to that in E_{direct}, has been elusive. For the low altitude sites (SGP and BOREAS) model calculations exceed measured by a substantial 19.6% ± 9.4% of measured $E_{diffuse}$ (Figure 7; references (11,13)). For 25 of the 40 cases investigated, this discrepancy is more than the combined uncertainties in model inputs and measurements. For days with relatively high inferred $\tau_{aerosol}$ (>0.2 at 550 nm), the modeled $E_{diffuse}$ was higher than measured; but in such cases the discrepancy could be explained by the presence of aerosols with lower than usual, but still within the uncertainty in its measurement of, single scattering albedo. When the $\tau_{aerosol}$ is high, $E_{diffuse}$ is sensitive to aerosol scattering properties. When the $\tau_{aerosol}$ is low, large reduction in ω_o and g are required to close the gap in $E_{diffuse}$. In the sensitivity analysis performed for a cloud-free day(13), modeled MODTRAN calculation of $E_{diffuse}$ (84 W m^{-2}) was found to be much higher than pyranometer measured offset corrected value (68 W m^{-2}) at a solar zenith angle of 40.29°. Only reducing measured ω_0 from 0.86 to 0.5, a value well below any reasonable estimate of uncertainty (usually 10%) is required to close the gap between model and measurement. No physically plausible values of g could close the gap. On the other hand, for a case with a relatively high $\tau_{aerosol}$ (0.24 at 550 nm), modeled value of $E_{diffuse}$ (147 W m^{-2}) could be made to agree with that measured (141 W m^{-2}) by reducing the ω_0 from a measured value of 0.92 to 0.89, a value within the uncertainty limit, or reducing g from the usual 0.7 to 0.55, still a reasonable value for rural aerosols. (Note that g=0.0 for Rayleigh scattering). Thus cloud-free days with high $\tau_{aerosol}$ are not suitable for

performing this closure experiment; those with low $\tau_{aerosol}$ on the other hand, are ideal.

Model overestimation in $E_{diffuse}$ under cloud-free skies has been observed by others(39,40,41,42,43). In addition to model overestimates of pyranometer measured $E_{diffuse}$, diffuse / total irradiance ratios are also overestimated(39) at many discrete bands in the shortwave. The diffuse/total ratios were measured by a multi-filter rotating shadow band radiometer(44). This instrument is superficially similar in configuration to a pyranometer but uses a silicon detector having a linear response over a wide range of intensities and negligible zero offset. Since ratios were used in this closure experiment, no calibration is required. Model overestimate of the diffuse / direct ratios is also found in the measurements of a rotating shadowband spectroradiometer (RSS, (42)) which has a continuous wavelength coverage (~500 channels) in the silicon part of the spectrum (0.360-1.1 μm).

At high altitude sites (MLO and SPO), MODTRAN calculates both E_{direct} and $E_{diffuse}$ to within the modeling and measurement uncertainties(11,13). Both these components were measured using instruments identical in construction to those used at low altitude sites and using identical calibration protocols (but independent procedures).

Why do models overestimate $E_{diffuse}$ while correctly calculating E_{direct}?

Closure in E_{direct} shows that (i) extinction is correctly measured in sunphotometer channels; (ii)Rayleigh extinction is correctly computed throughout the shortwave; (iii)models correctly compute gaseous absorption in between sunphotometer channels and (iv)models correctly interpolate and extend sunphotometer measured extinction in between and beyond sunphotometer channels. On the other hand, model overestimation of $E_{diffuse}$ shows that either molecular scattering and/or aerosol scattering may have been overestimated. Since Rayleigh scattering is estimated to an accuracy ~0.5% (corresponding to an optical thickness of 0.005), it must be concluded that the aerosol scattering has been overestimated and must be reduced to decrease the modeled $E_{diffuse}$. Reduction in aerosol scattering is accomplished by reducing $\tau_{aerosol}$. To conserve total extinction (for closure in E_{direct}) reduction in aerosol scattering must be accompanied by an increase in aerosol and/or gaseous absorption(13). *Kato et al.* (39) conjectured an additional gaseous absorption masquerading as aerosol optical thickness. The required atmospheric absorption (whether due to gases or aerosols) must be a continuum affecting more than one sunphotometer channel because if the absorption were localized in wavelength, it would have to be very strong to cause the observed discrepancy in $E_{diffuse}$. Given the amount of model overestimate, the required absorption is substantial (see below) and such an absorption, if localized in wavelength, would have been easily apparent.

Part of the optical thickness that has been routinely called as "aerosol optical thickness" in sunphotometry may have to be reassigned to an absorption process whose origin is yet unknown. Its wavelength dependence is also unknown. On some days almost all the so-called "aerosol optical thickness" has to be reduced to zero to achieve closure in $E_{diffuse}$. The wavelength dependence of $\tau_{aerosol}$ obtained on that day would approximately represent the required spectrum of the postulated excess absorption. It is found to have a dependence of λ^{-1} (Angstrom exponent of –1). For the many cases studied(11,13), this reduction in $\tau_{aerosol}$, $\Delta\tau$, is found to be an average 0.022 at 550 nm translating to an average excess absorptance of 5% (34 W m^{-2} day-side average for the Earth). Uncertainty of ±0.01 in optical thickness translates to an uncertainty of ±0.01 in $\Delta\tau$ as well. The corresponding uncertainty in absorptance is ±3%. It is to be understood that by "excess" is meant that the models currently do not have built

into them this additional atmospheric absorption, which they must include to correctly compute all the components of solar irradiance. Likewise models that infer 'true' $\tau_{aerosol}$ from sunphotometer measured τ_{total} must also identify and include a contribution from this excess absorptance.

How does the lack of closure in $E_{diffuse}$ affect closure in other components?

Preliminary calculations show that the required additional absorption in models affects all components except E_{direct} when sunphotometer data are used for estimating aerosol optical thickness. The problem can be remedied first by estimating the amount of excess absorption required to calculate measured $E_{diffuse}$, second, by assuming an Angstrom behavior for the optical thickness of the excess absorption with an exponent of –1, and third, by calculating part of the apparent aerosol optical thickness from sunphotometer measurements that is the real aerosol optical thickness. Wavelength dependence of the required additional absorption can also be obtained by an instrument such as the RSS. The 'true' $\tau_{aerosol}$ so determined could then be included in a forward calculation of the radiative transfer model to compute other components of the irradiance.

Some of the satellite sensor calibration procedures use approaches that in effect perform irradiance and radiance closure. For instance, in the irradiance method of performing ground-look calibration atmospheric and surface properties are adjusted in a radiative transfer model(45) to obtain closure in surface irradiance ($E_{diffuse}$ and $E^{\uparrow}_{diffuse}$) components. In the radiance based calibration, atmospheric and surface parameters are adjusted in the radiative transfer model to compute radiance at altitudes in the atmosphere to agree with accurate, aircraft based measurements(46). The model is then used to calculate at-sensor radiance, the required quantity for satellite sensor calibration. Given that there are two unknowns in the irradiance and radiance based methods – atmospheric absorption and surface reflectance - and given that the models have inadequate absorption built-in, it is not clear what, if any, effect will there be on the final computation of TOA at-sensor radiance. All previous ground-look calibrations are therefore suspect. For instance, preliminary calculations show that the more popular reflectance-based method will introduce errors of ~7% in satellite sensor calibration if additional absorption of ~5% absorptance is not included in the models(47).

CONCLUSIONS

Analysis of components of instantaneous shortwave irradiance on cloud-free days indicates possible serious shortcoming in the parameterization of key processes including atmospheric absorption in radiative transfer models. While E_{direct} is accurately computed by the models, $E_{diffuse}$ is overestimated. Overestimation in $E_{diffuse}$ is more than the uncertainty in model inputs and measurements; it is attributed to an atmospheric absorption process that is not accounted for in models that compute the irradiance components and in models that analyze sunphotometer measurements. At high altitudes using the same models and measurements that use identical instruments with similar calibration protocols, the agreement between models and measurements is within the mutual uncertainties. Thus, the absorption process is occurring at lower altitudes, perhaps in the boundary layer. Computation of upward irradiance at the surface and at TOA would be subject to closure problems as well. Satellite sensor calibration methods that depend on modeling at-sensor radiance would be affected. This includes all ground-look calibration (vicarious calibration) methods that are used to validate and supplement on-board calibration systems. It may be necessary to revisit satellite determination of important Earth-atmospheric radiative parameters such as albedo.

Acknowledgements

Funding from the Atmospheric Radiation Measurement Program of the U.S. Department of Energy, through Contract No. DE-AC02-98CH10886, is acknowledged for doing significant parts of this work.

REFERENCES

(1) Ohmura, A., E. G. Dutton, B. Forgan, C. Frohlich, H. Gilgen, H. Hegner, A. Heimo, G. Konig-Langlo, B. McAuthur, G. Muller, R. Philipona, R. Pinker, C. H. Whitlock, K. Dehne, and M. Wild, *BAMS, 79*, 2115-2136, 1998.

(2) Wiscombe, W. J., *Nature, 376*, 466-467, 1995.

(3) Lenoble, J., *Radiative Transfer in Scattering and Absorbing Atmospheres: Standard Computational Procedures*, A. Deepak Publishing, 1985.

(4) Fraser, R. S. and Y. J. Kaufman, *IEEE Trans. Geosci. Remote Sens.*, *GE-23, 5*, 625- 633, 1985.

(5) Nicodemus, F. E., J. C. Richmond, J. J. Hsia, I. W. Ginsberg, and T. Limperis, *NBS monograph 160*, 1977.

(6) Romero, J., N. P. Fox, and C. Frohlich, *Metrologia, 32*, 523-524, 1995/1996.

(7) Halthore, R. N., S. E. Schwartz, J. J. Michalsky, G. P. Anderson, R. A. Ferrare, B. N. Holben, and H. M. Ten Brink, *J. Geophys. Res., 102*, D25, 29,991- 30,002, 1997.

(8) Michalsky, J., E. Dutton, M. Rubes, D. Nelson, T. Stoffel, M. Wesely, M. Splitt, and J. DeLuisi, *J. Atmos. Ocean. Tech., 16*, 55-69, 1999.

(9) Forgan, B. W., *J. Atm. Ocean. Technol., 13*, 638-645, 1996.

(10) WMO, *Guide to Meteorological Instruments and Methods of Observation*, 6th Edition, World Meteorological Organization, 1995.

(11) Halthore, R. N. and S. E. Schwartz, *J. Geophys. Res.*, submitted, 1999.

(12) Cess, R. D., X. Jing, T. Qian, and M. Sun, *J. Geophys. Res.*, submitted, 1999.

(13) Halthore, R. N., S. Nemesure, S. E. Schwartz, D. G. Imre, A. Berk, E. G. Dutton, and M. H. Bergin, *Geophys. Res. Lttrs, 25*, 3591-3594, 1998.

(14) Bush, B. C., F. P. J. Valero, A. S. Simpson, and L. Bignone, *J. Atmos. Ocean. Technol.*, submitted, 1998.

(15) Charlock, T. P. and T. L. Alberta, *BAMS, 77* (11), 2673-2683, 1996.

(16) Bernstein L. S., A. Berk, P. K. Acharya, D.C. Robertson, G. P. Anderson, .J. H. Chetwynd, and L. M. Kimball, *J. Atmos. Sci., 53*, 2887-2904, 1996.

(17) Berk A., L. S. Bernstein, G. P. Anderson, P. K. Acharya, D. C. Robertson, J. H. Chetwynd, and S. M. Adler-Golden, *Remote Sens. Environ.*, in press, 1998.

(18) Wang, J., G. P. Anderson, H. E. Revercomb, and R. O. Knuteson, *Appl. Optics, 35*, 6028-6040, 1996.

(19) Kurucz, R. L., *Proc. 17th Ann. Rev. Conf. Atmos. Transmission Models*, G. P. Anderson, R. H. Picard, and J. H. Chetwynd, Eds., p. 332, Phillips Laboratory, Geophysics Directorate, MA, 1995.

(20) Neckel, H., and D. Labs, *Sol. Phys.*, *90*, 205-258, 1984.

(21) Lean, J., *Rev. Geophys.*, *29*, 505-535, 1991.

(22) Halthore, R. N. and B. L. Markham, *J. Geophys. Res., 97*, 18,731-18,742, 1992.

(23) Rothman, L. S., C. P. Rinsland, A. Goldman, S. Massie, D. P. Edwards, J.-M. Flaud, A. Perrin, C. Camy-Peyret, V. Dana, J.-Y. Mandin, J. Schroeder, A. McCann, R. R. Gamache, R. B. Wattson, K. Yoshino, K. V. Chance, K. W. Jucks, L. R. Brown, V. Nemtchinov and P. Varanasi, *JQSRT*, *60* (5), 1-89, 1998.

(24) Clough, S. A., F. X. Kneizys, and R. W. Davies, *Atmos. Res., 23*, 229-241, 1989.

(25) Slusser, J., X. Liu, K. Stamnes, G. Shaw, R. Smith, R. Storvold, F. Murcray, A. Lee, and P. J. Good, *J. Geophys. Res., 103*, 1549-1554, 1998.

(26) Tomasi, C., V. Vitale, and L. Tarozzi, *Nuovo Cimento, 20*, 61-88, 1997.

(27) Solomon, S., R. W. Portman, R. W. Sanders, and J. S. Daniel, *J. Geophys. Res., 103*, 3847-3858, 1998.

(28) Daniel, J. S., S. Solomon, R. W. Sanders, R. W. Portmann, and D. C. Miller, *J. Geophys. Res.*, in press, 1999.

(29) Bouguer, P., *Optical Treatise on the Gradation of Light*. 1725. Translated with introduction and notes by W. E. Knowles Middleton, Univ. of Toronto Press, 1961.

(30) Holben, B. N., T. F. Eck, I. Slutsker, D. Tanre, J. P. Buis, A. Setzer, E. Vermote, J. A. Reagan, Y. J. Kaufman, T. Nakajima, F. Lavenu, I. Jankowiak, and A. Smirnov, *Rem. Sens. Environ., 66*, 1-16, 1998.

(31) Schmid, B., J. J. Michalsky, R. N. Halthore, M. C. Beauharnois, L. C. Harrison, J. M. Livingston, P. B. Russell, B. N. Holben, T. F. Eck, and A. Smirnov, *Geophys. Res. Lttrs*, in press, 1999.

(32) Anderson, T. L., D. S. Covert, S. F. Marshall, M. L. Laucks, R. J. Charlson, A. P. Waggoner, J. A. Ogren, R. Caldow, R. L. Holm, F. R. Quant, G. J. Sem, A. Wiedensohler, N. A. Ahlquist, and T. S. Bates, *J. Atm. Ocean. Tech., 13*, 967-986, 1996.

(33) Heintzenberg, J. and R. J. Charlson, *J. Atmos. Ocean. Technol., 13*, 987-1000, 1996.

(34) Marshall, S. F., D. S. Covert, and R. J. Charlson, *App. Opt., 34*, 6306-6311, 1995.

(35) Lin, C. L., M. B. Baker, and R. J. Charlson, *Appl. Optics, 12*, 1356-1363, 1973.

(36) Clarke, A. D., K. J. Noone, J. Heintzenberg, S. G. Warren, and D. S. Covert, *Atmos. Environ., 21* (6), 1455-1465, 1987.

(37) Deering, D. W., E. M. Middleton, and T. F. Eck., *Rem. Sens Env., 47*, 242-260, 1994.

(38) Peixoto, J. P. and A. H. Oort, *Physics of Climate*, American Institute of Physics, New York, NY, 1992.

(39) Kato, S., T. P. Ackerman, E. E. Clothiauk, J. H. Mather, G. G. Mace, M. L. Wesely, F. Murcray, and J. Michalsky, *J. Geophys. Res., 102*, 25,881-25,898, 1997.

(40) Fu, Q., G. Lesins, W. B. Sun, and J. Higgins, *Proc. of the 8th Atmospheric Radiation Measurement (ARM) Science Team Meeting*, pp. 271-276, DOE/ER-0738, U.S. Dept. of Energy, Washington, DC, 1998.

(41) Trishchenko, A. and Z. Li, *Proc. of the 8th Atmospheric Radiation Measurement (ARM) Science Team Meeting*, pp. 761-765, DOE/ER-0738, U.S. Dept. of Energy, Washington, DC, 1998.

(42) Harrison, L., M. Beauharnois, J. Berndt, P. Kiedron, J. Michalsky, and Q. Min, *Geophys. Res. Lttrs*, submitted, 1999.

(43) Ricchiazzi, P., C. Gautier, and T. P. Tooman. Presented at the 9th Atmospheric Radiation Measurement Science Team Meeting, San Antonio, TX, March 1999.

(44) Harrison, L., J. Michalsky, and J. Berndt, *Appl. Opt., 22*, 5118-5125, 1994.

(45) Slater, P. N., S. F. Biggar, K. J. Thome, D. I. Gellman, and P. R. Spyak, *J. Atmos. Ocean. Tech., 12*, 349-359, 1996.

(46) Abel, P., R. G. R. Smith, R. H. Levin and H. Jacobowitz, SPIE, 924, 1988.

(47) Halthore, R. N., A. T. Cialella, B. L. Markham, and J. Seiferth, Presented at the 9th Atmospheric Radiation Measurement Science Team Meeting, San Antonio, TX, March 1999.

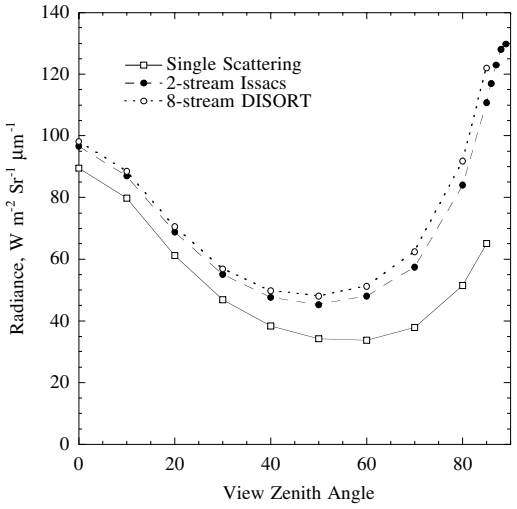

Figure 1. Model computed radiance is plotted as a function of zenith angle for an overhead Sun. Results of three models are shown here-single scattering, two stream Issacs model, and an 8 stream model based on discrete ordinate method. All three models are available in MODTRAN. This figure shows that even for the relatively clean atmospheric conditions used as inputs to models, the difference between multiple scattering and single scattering is quite large especially at large zenith angles.

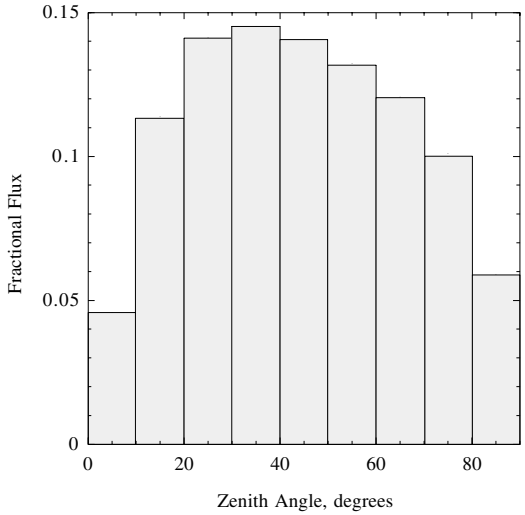

Figure 2. Fractional flux, defined as fractional contribution of radiance from a 10˚ zenith angle interval and all azimuth angles to the total surface irradiance, is plotted as a function of zenith angle. Thus the contribution of radiance from a slice of the sky between 40 and 50˚ is about 0.14 toward DFDI at 550 nm. Likewise the contribution of sky radiance between 80 and 90˚ is 0.06 or 6% toward DFDI. Radiance from Figure 1 for the 2 stream case is used here.

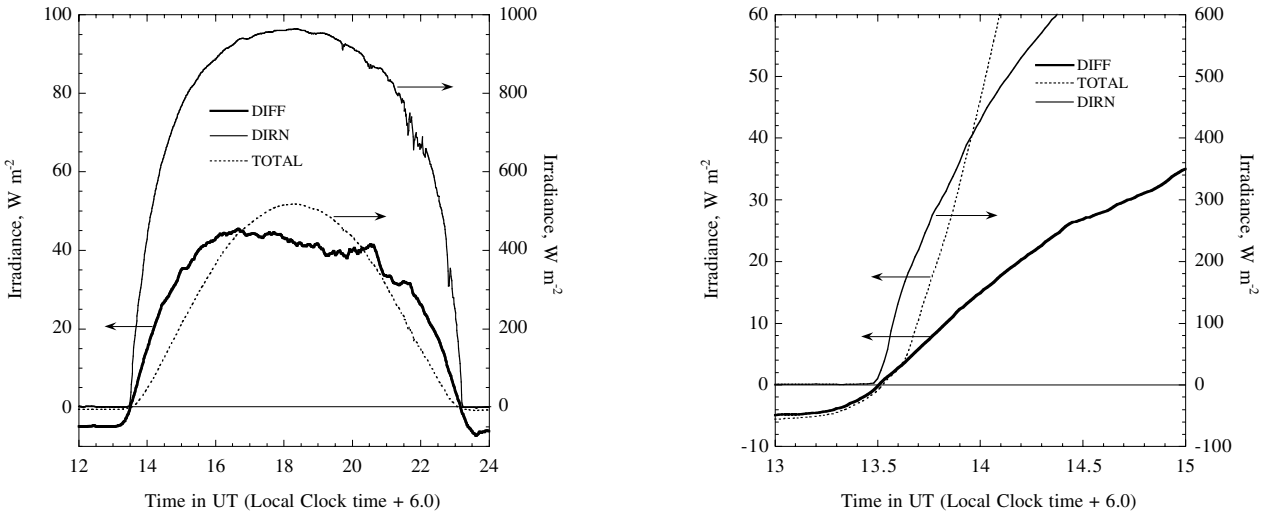

Figures 3 and 4. E_{direct} (identified as DIRN), $E_{diffuse}$ (DIFF), and E_{total} (TOTAL) measured by a pyrheliometer, shaded pyranometer and a pyranometer respectively, are shown for a cloud-free day (December 8, 1996) at United States Department of Energy's (DOE) Atmospheric Radiation Measurement (ARM) site in Oklahoma (latitude: 36.605˚ N; longitude: 97.485˚ W; altitude: 315 m). Figure 4 expands the sunrise portion of Figure 3 to clearly depict the negative offset values at sunrise and at night in both the E_{total} and $E_{diffuse}$ values. Time of sunrise is identified by a rapid increase in the E_{direct}.

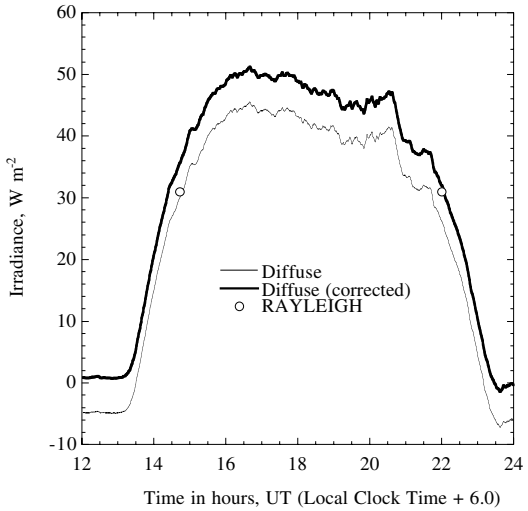

Figure 5. It is necessary to correct for the observed offsets in pyranometers. Uncorrected diffuse irradiance (same as that in Figure 4) is found to be less than that calculated for a purely Rayleigh atmosphere (circles) in both morning and evening. This is an impossible circumstance since Rayleigh calculation represents minimum diffuse brightness of the atmosphere. After correction for the zero offset, the measured values are higher. Diurnal asymmetry is present because of changes in aerosol optical thickness, in particular aerosol scattering.

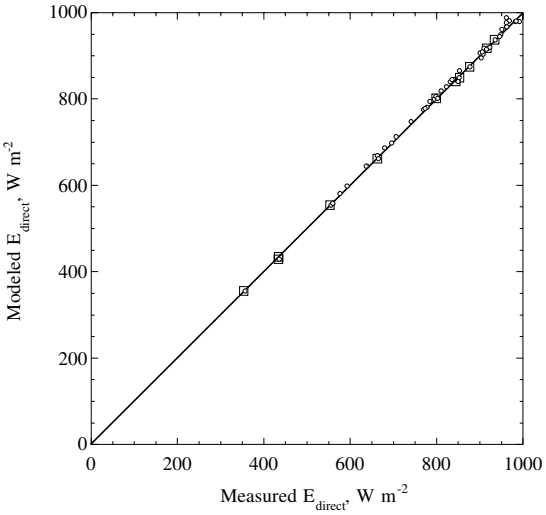

Figure 6. MODTRAN calculated E_{direct} plotted against that measured (ACR, squares; pyrheliometer, circles) shows agreement to within 0.012% ± 0.45% for 11 comparisons with ACR and –0.4% ± 0.82% for 49 comparisons with pyrheliometers. Data span a period from 1996 to 1998 at the SGP. The agreement is well within the uncertainties in measurements and model inputs.

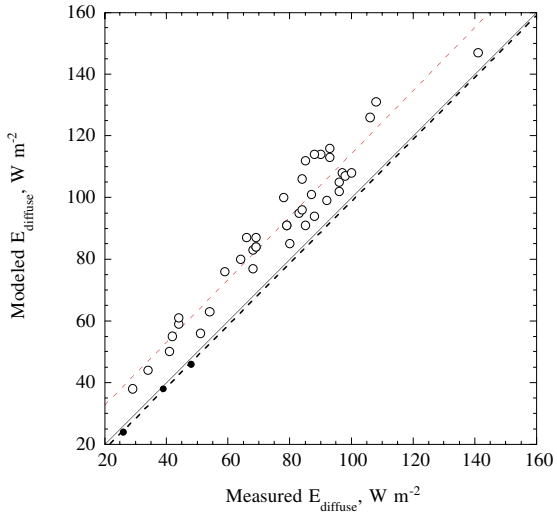

Figure 7. MODTRAN computed $E_{diffuse}$ is plotted against that measured for two low altitude sites (open circles, 39 cases) and two high altitude sites (filled circles, 3 cases). Dashed lines represent least-squared fits to data. Model overestimation is clearly apparent for low altitude sites in this figure (19.6% ± 9.4%) with 25 cases out of 39 showing an overestimate beyond modeling and measurement uncertainties(11). For high altitude sites the agreement (-4.8% ± 2.6%) is well within the uncertainties in measurements and model inputs (±12%). Data from 1994 to 1997 and from all 4 sites-SGP, BOREAS, MLO and SPO, are shown here with each data point representing an independent closure experiment with unique set of model inputs and measurements.